Cell. Mol. Life Sci. (2010) 67:829–840
DOI 10.1007/s00018-009-0218-9

Cellular and Molecular Life Sciences

RESEARCH ARTICLE

Differential water permeability and regulation of three aquaporin 4 isoforms

Robert A. Fenton · Hanne B. Moeller · Marina Zelenina · Marteinn T. Snaebjornsson · Torgeir Holen · Nanna MacAulay

Received: 29 September 2009 / Revised: 3 November 2009 / Accepted: 16 November 2009 / Published online: 15 December 2009

Abstract Aquaporin 4 (AQP4) is expressed in the perivascular glial endfeet and is an important pathway for water during formation and resolution of brain edema. In this study, we examined the functional properties and relative unit water permeability of three functional isoforms of AQP4 expressed in the brain (M1, M23, Mz). The M23 isoform gave rise to square arrays when expressed in *Xenopus laevis* oocytes. The relative unit water permeability differed significantly between the isoforms in the order of M1 > Mz > M23. None of the three isoforms were permeable to small osmolytes nor were they affected by changes in external K^+ concentration. Upon protein kinase C (PKC) activation, oocytes expressing the three isoforms demonstrated rapid reduction of water permeability, which correlated with AQP4 internalization. The M23 isoform was more sensitive to PKC regulation than the longer isoforms and was internalized significantly faster. Our results suggest a specific role for square array formation.

Keywords Aquaporin · Glial cells · Water permeability · Regulation · Protein kinase C · Isoforms

All authors belong to Nordic Center of Excellence for Water Imbalance Related Disorders.

Electronic supplementary material The online version of this article (doi:10.1007/s00018-009-0218-9) contains supplementary material, which is available to authorized users.

R. A. Fenton · H. B. Moeller
The Water and Salt Research Center, Department of Anatomy, University of Aarhus, 8000 Aarhus, Denmark

M. Zelenina
Department of Women's and Children's Health, Karolinska Institutet, 171-77 Stockholm, Sweden

M. Zelenina
Department of Applied Physics, Royal Institute of Technology, Stockholm, Sweden

M. T. Snaebjornsson
Department of Anatomy, University of Iceland, Reykjavik, Iceland

M. T. Snaebjornsson · T. Holen
Department of Anatomy, University of Oslo, PO Box 1105, Blindern, 0317 Oslo, Norway

N. MacAulay (✉)
Department of Cellular and Molecular Medicine, The Panum Institute, University of Copenhagen, Blegdamsvej 3, 12.6, 2200 Copenhagen, Denmark
e-mail: macaulay@sund.ku.dk

Introduction

Aquaporin 4 (AQP4) is the principal water channel in the central nervous system. It is predominantly expressed in areas with close contact to the blood vessels or to the cerebrospinal fluid, such as the pericapillary glial endfeet and the ventricular ependymal cell lining, in which fluid exchange takes place between the brain and the blood/cerebrospinal fluid [1, 2]. The distinct polarized expression of AQP4 appears to be promoted by the basal lamina-associated extracellular matrix component, agrin [3]. During pathophysiological conditions leading to brain edema, AQP4 plays a role in the underlying brain water accumulation, either by permitting water entry into the brain parenchyma or by allowing accumulated water to exit, depending on whether the edema is of cytotoxic or vasogenic origin (reviewed in [4]).

AQP4 in brain tissue, cultured primary astrocytes, or expressed in various heterologous expression systems is

reported to be regulated by numerous protein kinases, such as protein kinase C (PKC), protein kinase A (PKA), Ca^{2+}/calmodulin-dependent kinase II (CamKII), casein kinase II (CKII), and protein kinase G (PKG) [5–11]. Phosphorylation-dependent regulation of AQP4 might thus encompass several processes, including gating, protein internalization, lysosomal targeting, and Golgi transition.

Three of the AQP4 isoforms have been demonstrated to transport water: M1 (AQP4a) consisting of 323 amino acids, the shorter M23 (AQP4c) consisting of 301 amino acids, and Mz (AQP4e) consisting of 364 amino acids [12–14]. M23 is the prevalent isoform in the mammalian brain [15] and gives rise to the square arrays detected in the astrocytic endfeet [16–18]. The isoform composition of these square arrays is currently debated [19–21]. Co-transfection of the M1 and M23 isoforms modulate the size of square arrays [16], possibly due to palmitoylation of two cysteines at positions 13 and 17, which are lacking in the shorter M23 isoform [21, 22]. The importance of these two residues for square array formation was recently challenged and new molecular determinants put forth [23].

The rationale for endogenous expression of distinct isoforms of AQP4 in the brain and the function of square arrays have remained elusive, although the adhesive properties of AQP4 between adjoining membranes expressing the M23 isoform may provide a possible explanation [24]. Previously, two conflicting reports have estimated the unit water permeability of M1 and M23 to be either identical [15] or eightfold higher in M23 compared to M1 [25]. In this study, we aimed to resolve this discrepancy, in addition to investigating possible differences in the permeability profile and phosphorylation-dependent regulation of all three AQP4 isoforms.

Materials and methods

Oocyte preparation and expression of AQP4 isoforms

Xenopus laevis frogs were obtained from Nasco (USA) or National Center for Scientific Research (France). After surgical removal of the oocytes from anesthetized frogs, the follicular membrane was removed by incubation in Kulori medium (90 mM NaCl, 1 mM KCl, 1 mM $CaCl_2$, 1 mM $MgCl_2$, 5 mM HEPES, pH 7.4, 182 mOsm) containing 10 mg/ml collagenase (type 1; Worthington, NJ, USA) and trypsin inhibitor (1 mg/ml; Sigma, Denmark) for 1 h. Subsequently, the oocytes were washed five times in Kulori medium containing 0.1% bovine serum albumin (Sigma) and incubated in 100 mM K_2HPO_4 with 0.1% BSA for 1 h. After the final oocyte collection, the frogs were anesthetized and killed by decapitation. The protocol complies with the European Community guidelines for the use of experimental animals, and the experiments were approved by The Danish National Committee for Animal Studies. The three isoforms of rat AQP4 (AQP4a, AQP4c, and AQP4e) will in the remainder of the paper be referred to as M1, M23, and Mz, respectively. Note that it is not fully resolved whether the AQP4e cDNA encodes the Mz band detected in brain lysate [14]. The cDNAs encoding the isoforms in the oocyte expression vector pXOOM were linearized downstream from the poly-A segment, and in vitro transcribed using mMessage Machine according to manufacturer's instruction (Ambion). cRNA was extracted with MEGAclear (Ambion) and microinjected into defolliculated *Xenopus* oocytes (25 ng RNA/oocyte).

Freeze fracture electron microscopy

AQP4-expressing oocytes were fixed in 0.1 M sodium cacodylate (NaCac), 2.5% glutaraldehyde, pH 7.4 for 80 min with slow shaking and subsequently stored in 0.12 M NaCac, 34% glycerol, 0.12% gluteraldehyde at 4°C. Freeze fracture was performed essentially as previously described [26]. In brief, fixed oocytes were equilibrated overnight in 25% glycerol at 4°C, attached to gold holders, and snap frozen in Freon 22 cooled in liquid nitrogen. Oocytes were fractured in a Balzer's freeze fracture apparatus (BAF 300; Balzers) at −100°C. Samples were immediately rotary shadowed at an angle of 25° with platinum and carbon replicated. The replicas were cleaned overnight in 40% chrome oxide, rinsed with water, and analyzed with a CM100 TEM microscope (FEI).

Blue native gel electrophoresis (BN-PAGE) of AQP4 isoforms expressed in HeLa cells and *Xenopus* oocytes

HeLa cells were grown in 75-cm^2 culture flasks using Dulbecco's modified Eagle medium (DMEM; Invitrogen) supplemented with 10% fetal bovine serum (FBS; Gibco) and 1% L-glutamine (Lonza). At 24 h prior to transfection, cells were seeded at a density of 20,000 cells/cm^2. FuGENE6 transfection reagent (Roche) was used at the ratio of 3:1 (FuGENE6:DNA) in accordance with the manufacturer's instructions. Then, 24 h post-transfection cells were trypsinized and suspended in 9 ml of medium before centrifugation at 1,000*g* for 10 min. Subsequently, cells were washed in 10 ml of phosphate buffered saline (PBS) and centrifuged again at 1,000*g* for 10 min. Cells from one 75-cm^2 culture flask were homogenized in 200 µl of HEPES buffer (10 mM HEPES, pH 7.4, 2 mM EDTA, 333 mM sucrose, and complete protease inhibitor cocktail; Roche) using cold mortar and pestle. The lysate was centrifuged at 1,000*g* for 10 min and the supernatant used for BN-PAGE electrophoresis. *Xenopus* oocytes and cerebellum from rat were homogenized in the HEPES buffer in the

ratio 1:10 (mg tissue: µl buffer) and the lysate was then treated as described above for the cell lysate. Next, 2–10 µg of total protein sample was mixed with 4× native PAGE sample buffer (Invitrogen) and 5% dodecyl β-D-maltoside (DDM) to a final concentration of 1× sample buffer and 1% DDM in a volume of 20 µl. Samples were incubated at RT for 10 min and then centrifuged for 10 min at 10,000*g*. After centrifugation, the supernatant was mixed with Coomassie G-250 1:4 (Coomassie G-250:DDM). Samples were loaded on a 4–16% BN-PAGE Bis–Tris gradient gel. NativeMark unstained protein standard (Invitrogen) was used as a molecular weight marker. Electrophoresis was carried out at 150 V, with the dark cathode buffer (5% 20× running buffer and 5% cathode additive; both Invitrogen) for the first 20 min, and with the light cathode buffer (5% 20× running buffer, 0.5% cathode additive) for the next 140 min. The anode buffer was the same as the cathode buffer but contained no cathode additive. Gels were then blotted to PVDF membranes and probed with AQP4 antibodies, as described previously [20].

Osmotic water permeability measurements on *Xenopus* oocytes

The osmotic water permeability measurements were performed as previously described [27]. During the measurements, the membrane potential of the oocytes was measured by two-electrode voltage clamp with a Dagan Clampator interfaced to an IBM-compatible PC using a Digidata 1322 A/D converter and pClamp 9.2 (Axon Instruments). The oocyte was placed in a small chamber with a glass bottom, through which the oocyte could be viewed via a long distance objective (×4) and a CCD camera. To quantify the oocyte volume changes, oocyte images were captured and processed as previously described in detail [27]. The experimental chamber was perfused by a control solution (100 mM NaCl, 2 mM KCl, 1 mM $CaCl_2$, 1 mM $MgCl_2$, 10 mM HEPES, pH 7.4) and hypertonic test solution which was obtained by adding 20 mOsm of mannitol to the control solution. For measurements of the reflection coefficients, the mannitol was replaced with equiosmolar urea, glycerol, or formamide. Osmolarities of the test solutions were determined with an accuracy of 1 mOsm by a cryoscopic osmometer (Gonotec, Berlin, Germany). For the experiments with 8 mM K^+, the control 2 mM K^+ solution contained an additional 6 mM choline chloride to keep the two control solutions equiosmolar. Phorbol 12-myristate 13-acetate (PMA) was obtained from Sigma–Aldrich. The osmotic water permeability is given in units of (cm/s) and was calculated as $L_p = -J_v/A \times \Delta\pi \times V_w$, where J_v is the water flux during the osmotic challenge, A is the true membrane surface area (about nine times the apparent area due to membrane foldings [28]), $\Delta\pi$ is the osmotic challenge, and V_w is the partial molal volume of water, 18 cm^3/mol.

Immunoblotting on *Xenopus* oocytes

The preparation of oocyte plasma membranes was modified from [29] and has been recently described in detail [30]. In brief, total oocyte membranes were obtained by homogenization (with a p200 pipette) of two oocytes in 1 ml HbA+ buffer: 5 mM $MgCl_2$, 5 mM NaH_2PO_4, 1 mM EDTA, 80 mM sucrose, 20 mM Tris, pH 7.48, containing the protease inhibitors leupeptin (8 µM) and pefabloc (0.4 mM). The supernatant was recovered following 10 min centrifugation at 250*g* and subsequently centrifuged at 14,000*g* for 20 min to obtain the total membrane fraction. The pellets were resuspended in 20 µl HbA+ followed by addition of 5 µl of 5× sample buffer (7.5% SDS, 250 mM Tris (pH 6.8), 30% glycerol, bromphenol blue, and 60 mg/ml DTT) and heated at 65°C for 15 min. Plasma membranes were obtained from a minimum of 15 oocytes for each construct/condition. The oocytes were treated as previously described [29] prior to homogenization and consecutive centrifugation steps [30]. Total oocyte membranes and purified plasma membranes were subjected to immunoblotting using rabbit polyclonal anti-AQP4 antibody (Alamone Labs, Israel), 1:1,000. Sites of antibody–antigen reaction were visualized using an enhanced chemiluminescence substrate (GE Healthcare, Denmark) before exposure to light-sensitive film. Numerous film exposures were performed to be certain that the linearity of the film was not exceeded. The band densities were quantified by densitometry.

Immunocytochemistry and confocal laser scanning microscopy on *Xenopus* oocytes

The oocytes were fixed for 1 h in 3% paraformaldehyde in Kulori medium, rinsed in Kulori medium, dehydrated in a series of ethanol concentrations (40 min in 70, 96, and 99% ethanol) and incubated in xylene for 1 h. Oocytes were infiltrated with paraffin for 1 h at 50°C before embedding. Next, 2-µm sections were cut on a Leica RM 2126 microtome and immunostained as described previously [31] using rabbit polyclonal anti-AQP4 antibody. An Alexa 488-conjugated secondary antibody was used for visualization (DAR; Invitrogen). A Leica TCS SL confocal microscope and Leica confocal software were used for imaging of the oocytes. Control AQP4-expressing oocytes were used to set laser intensity and capture settings on the microscope such that saturation of images for each condition was avoided. The microscope and laser settings were kept constant within each experiment. Images were taken

using an HCX PL APO ×63 oil objective lens. A minimum of two images per oocyte, with 3–5 oocytes per experiment, were used for statistical analysis. Image semi-quantification and validation has recently been described in detail [30]. To facilitate comparisons between experiments and between individual oocytes, plasma membrane fluorescence was normalized to total oocyte fluorescence.

Water permeability measurements in mammalian cells

A human bronchial epithelial cell line BEAS-2b (European Collection of Cell Cultures, Center for Applied Microbiology and Research, Salisbury, Wiltshire, UK; subpassages 8–16) was cultured on coverslips (Bioptechs, Butler, PA) coated with collagen type I and fibronectin (Sigma–Aldrich Sweden) in Dulbecco's MEM/NUT MIX F-12 (1:1) medium (Gibco, Paisley, Scotland, UK) containing 0.5 U/ml penicillin, 50 μg/ml streptomycin, and supplemented with 10% heat-inactivated FBS and 2 mM L-glutamine. On the second day of culture, the cells were transiently transfected using CLONfectin (Clontech) according to the manufacturer's protocol. cDNA constructs used for the transfection were described previously [32]. cDNA fragments encoding human AQP4 M1 and AQP4 M23 were subcloned into the pIRES2-EGFP vector (Clontech). The resulting constructs expressed AQP4 and GFP as separate proteins in the same cell. Experiments were performed on the fourth day of culture. Cells positive for AQP4 M1 and M23 were identified by GFP fluorescence. The GFP signal was distributed evenly in the cytoplasm of the cells. The cells positive for AQP4 M1 and M23 were not different in morphology compared to each other or to the untransfected cells.

Water permeability of the cells was measured as previously described [7, 11, 33]. Briefly, the cells were mounted in a closed chamber on the stage of an inverted confocal laser scanning microscope in isoosmotic, 300 mOsm PBS. The cells were loaded with 20 μM calcein-AM (Molecular Probes; Invitrogen) for 5 min at RT. Loading with calcein was similar in transfected and untransfected cells. The cells were perfused with isosmotic PBS and scanned every 1.8 s with excitation at 488 nm. The fluorescent signal was collected at 515–525 nm from an optical slice within the cell body. The cells were then subjected to an osmotic shock by switching the perfusate to a hypoosmotic, 200 mOsm, PBS, obtained by omission of 50 mM NaCl from the isosmotic solution. The swelling of the cells was monitored as a decrease of calcein fluorescence, which occurred due to the dilution of the fluorophore and a reduction in self-quenching. The initial slope of the fluorescence intensity curve was used to calculate water permeability (P_f) of each cell as described in detail previously [7, 11, 32, 33]. The P_f of all cells in each experiment was expressed relative to the mean maximal P_f in cells transfected with M1.

Osmolyte uptake measurements in *Xenopus* oocytes

The uptake of osmolytes was measured using radioactively labeled compounds. The experiments were performed in 24-well plates (five oocytes/condition) containing 500 μl test solution (100 mM NaCl, 2 mM KCl, 1 mM $CaCl_2$, 1 mM $MgCl_2$, 10 mM HEPES, pH 7.4) containing 20 mOsm of the unlabeled osmolyte and trace amounts of [^{14}C]mannitol, [^{14}C]urea, [^{14}C]glycerol, or [^{14}C]formamide (Amersham, UK). The oocytes were pre-incubated in control solution containing 20 mOsm of non-permeable sucrose in order to avoid imposing an osmotic challenge at the initiation of the uptake experiment. The oocytes were incubated in the test solution for 5 min at RT with gentle shaking, washed four times in ice-cold test solution without the radioactive osmolytes, and dissolved individually in 200 μl 10% SDS. Finally, 2 ml scintillation fluid (Opti-fluor; Packard, Netherlands) was added and the samples counted in a scintillation counter (Packard Tri-Carb).

Data are presented as mean ± SE for n = number of cells. Student's t test has been used for the statistical analysis.

Results

Three isoforms of AQP4 (M1, M23, and Mz) were individually expressed in *Xenopus* oocytes to investigate possible differences in their functional properties. This expression system is widely used to assess relative unit water permeability and solute permeability of different aquaporins (see, e.g., [30, 34]). Expression of the AQP4 isoforms increased the water permeability of the oocytes from (in $\times 10^{-3}$ cm/s) 0.10 ± 0.01 ($n = 19$) for the non-injected oocytes to 1.47 ± 0.05 ($n = 37$) for M1, 1.60 ± 0.11 ($n = 37$) for M23, and 1.31 ± 0.06 ($n = 37$) for Mz.

Formation of square arrays

To validate the use of *Xenopus* oocytes as an expression system for this comparative study, we explored the ability of AQP4 isoforms to form square arrays in oocytes by performing freeze fracture electron microscopy. As shown in Fig. 1a, b, and c, highly ordered structures characteristic of square arrays were visible in M23-expressing oocytes (P-face as well as E-face). These arrays were only apparent at the oocyte plasma membrane (electronic

supplementary material, Fig. 1). Due to the extensive invaginations of the *Xenopus* oocyte membrane [28], only sporadic patches of plasma membrane were in the plane of the fracture, which excluded quantitative studies of the array formation. No ordered structures were observed in oocytes expressing M1 and Mz (Fig. 1d, e). In addition, we analyzed M1-, M23-, and Mz-expressing oocytes using blue native poly-acryl gel electrophoresis (BN-PAGE) that was recently established as a biochemical assay to visualize AQP4 higher order structures [20]. As shown in Fig. 1f, the M23 isoform, whether heterologously expressed in HeLa cells or *Xenopus* oocytes, gave rise to the higher order structures that are the hallmark of the square arrays and also apparent in rat cerebellum. The M1 and Mz isoforms did not form higher order structures when expressed in HeLa cells or in *Xenopus* oocytes. Thus, in *Xenopus* oocytes, AQP4 assembles similarly to native tissue, making oocytes a suitable model for functional studies.

Relative unit water permeability of AQP4 isoforms expressed in *Xenopus* oocytes

The relative unit water permeability of M1 and M23 is debated [15, 25] and we therefore set out to resolve this issue. We have recently established sensitive methods to estimate the relative unit water permeability of different aquaporins [30] in which the water permeability of the AQP-expressing oocyte is normalized to the abundance of the AQP in the oocyte plasma membrane. We determined the water permeability of oocytes expressing M1, M23, or Mz by exposing the oocytes to an osmotic challenge of 20 mOsm mannitol (added to the control solution) (Fig. 2a). The water permeability of the native oocyte membrane (<10% of the total L_p) was deducted in order to obtain the contribution from each AQP4 (in $\times 10^{-3}$ cm/s): 1.15 ± 0.04 for M1 ($n = 25$), 1.17 ± 0.09 for M23 ($n = 25$), and 1.07 ± 0.05 for Mz ($n = 20$) for a total of 4–5 batches, which were not significantly different from

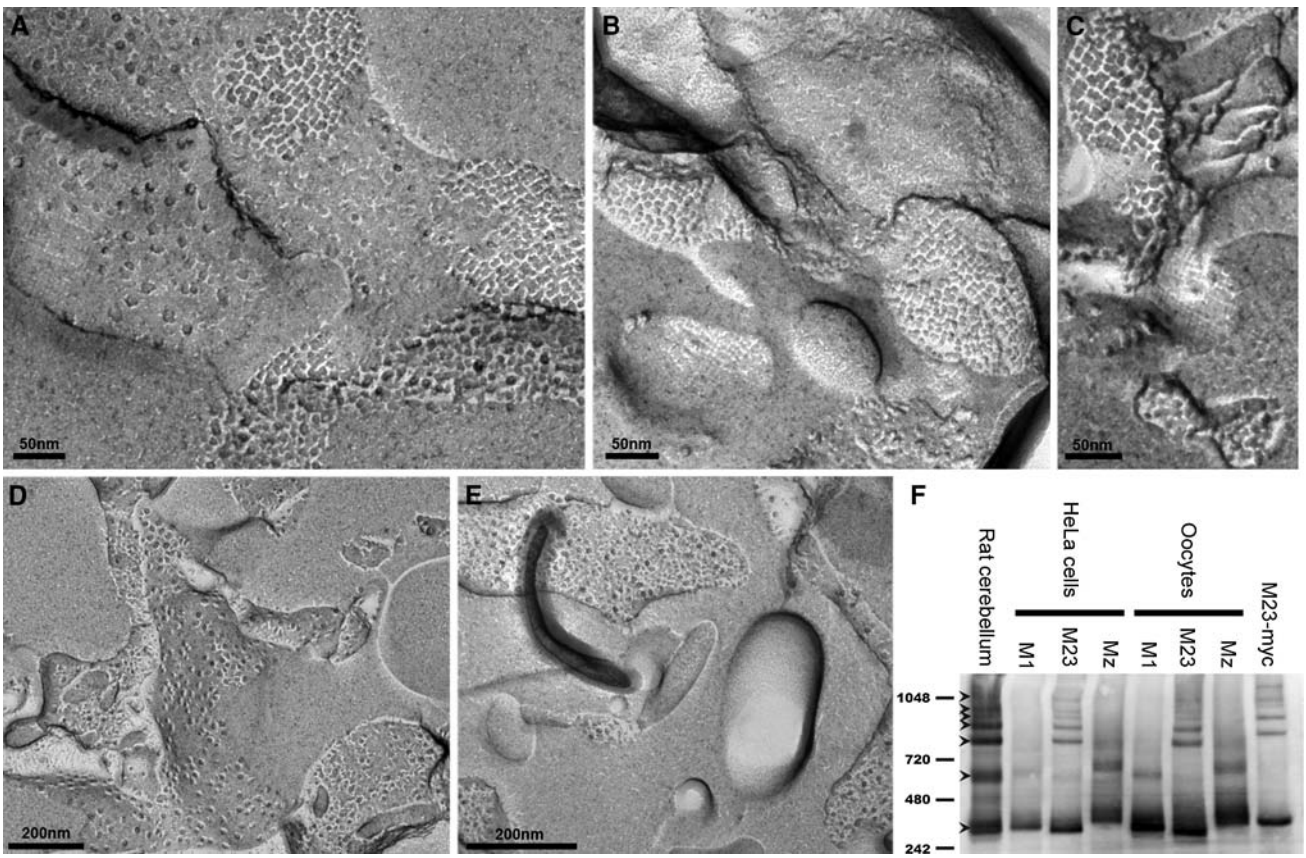

Fig. 1 The M23 isoform forms square arrays in *Xenopus laevis* oocytes. **a–c** At the plasma membrane, highly ordered structures characteristic of square arrays are observed for the M23 isoform. In contrast, neither the M1 isoform (**d**) nor the Mz isoform (**e**) show similar ordered structures. **f** BN-PAGE analysis of AQP4. In contrast to the M1 and Mz isoforms, the M23 isoform forms higher molecular weight moieties in both HeLa cells and *Xenopus* oocytes. *Lane 1* brain lysate (rat cerebellum), *lanes 2–4* M1, M23, and Mz expressed in HeLa cells, *lanes 5–7* M1, M23, and Mz expressed in *Xenopus* oocytes. Control M23-myc expressed in HeLa cells also exhibited higher order bands (*lane 8*). Molecular weight markers are indicated to the *left*, in kDa. The lower tetramer band and six higher order bands are indicated by *arrowheads*

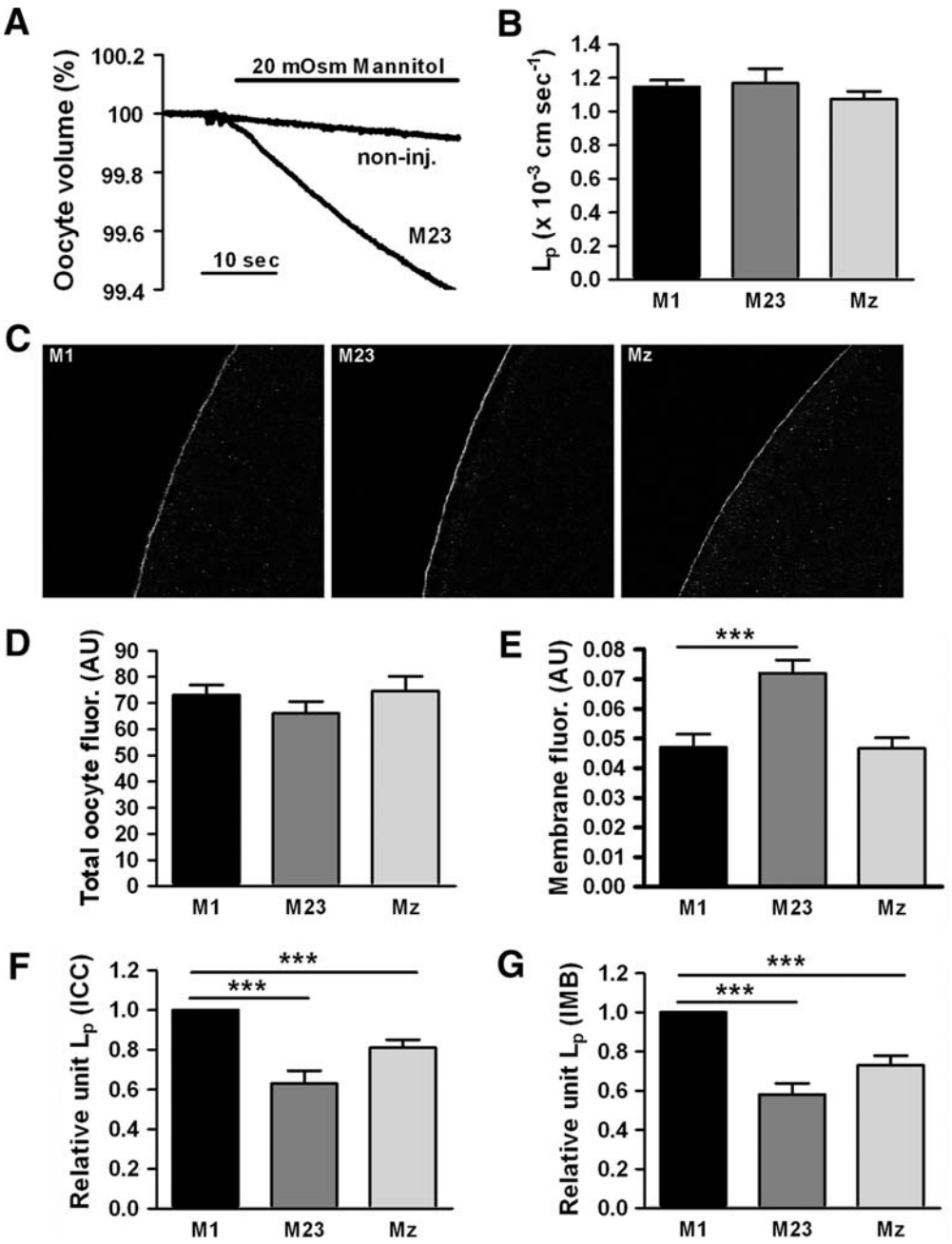

Fig. 2 The relative unit water permeability of M1, M23, and Mz expressed in oocytes. **a** An oocyte expressing the M23 isoform and a non-injected oocyte (with L_ps of 1.14 and 0.11×10^{-3} cm/s, respectively) were challenged with an osmotic gradient of 20 mOsm mannitol for 30 s. **b** The average water permeability of oocytes expressing M1, M23, or Mz with the contribution of the native oocyte membrane deducted ($n = 20$–25 of each). **c** Representative confocal laser scanning microscopy of oocytes expressing M1, M23 and Mz immunolabeled for AQP4. **d** Oocyte total fluorescent counts (in arbitrary units) were used to asses the abundance of AQP4 in oocytes expressing the three isoforms ($n = 15$–20 of each). **e** Oocyte plasma membrane fluorescent counts (in arbitrary units) were used to asses the AQP4 abundance in the plasma membrane of oocytes expressing the three isoforms ($n = 15$–20 of each). **f** Normalized relative unit water permeability of the three isoforms based on quantification by immunocytochemistry ($n = 4$–5 experiments based on 3–5 oocytes of each). **g** Normalized relative unit water permeability of the three isoforms based on quantification by immunoblotting of purified plasma membranes ($n = 3$ experiments, each based on $n = 5$ oocytes of each isoform for the L_p determination and $n = 20$ oocytes of each isoform for the plasma membrane purification). ***$P < 0.001$ (compared to M1)

each other (Fig. 2b). Subsequently, we determined the relative abundance of AQP4 protein in each oocyte (total abundance and plasma membrane abundance) by immunolabeling of the same oocytes employed for the L_p measurements using an anti-AQP4 antibody that recognizes the C-terminal part of the protein. Representative confocal images of the immunostained oocytes are shown in Fig. 2c. Semi-quantification of the images for each isoform revealed a similar amount of total fluorescent counts corresponding to total AQP4 protein in the oocytes (Fig. 2d), whereas the plasma membrane abundance differed between the isoforms, with M23 demonstrating a significantly larger fraction of the total protein in the plasma membrane ($P < 0.001$): (in arbitrary units, average of all oocytes used in the 4–5 batches of oocytes used in the dataset): 0.047 ± 0.004 for M1 ($n = 20$), 0.072 ± 0.004 for M23 ($n = 18$), and 0.047 ± 0.004 for Mz ($n = 18$) (Fig. 2e).

To compare the unit water permeability of the three isoforms, the water permeability relative to the plasma membrane abundance was calculated for *each* experiment (batch of oocytes) after which it was normalized to M1 and

then averaged. As shown in Fig. 2f, the relative unit water permeability of M23 was significantly lower than M1 ($P < 0.001$). The relative unit water permeability of Mz was intermediate and significantly lower than M1 ($P < 0.001$): 1.00 ± 0.00 for M1, 0.63 ± 0.07 for M23, and 0.81 ± 0.04 for Mz ($n = 4$–5 experiments with 3–5 oocytes expressing each isoform). To verify these results, we performed immunoblotting of total oocyte membranes and purified plasma membranes from M1-, M23-, and Mz-expressing oocytes day-matched with water permeability measurements on the same batch of oocytes. The total expression of AQP4 was similar for M1-, M23-, and Mz-expressing oocytes (data not shown) but in accordance with the immunostaining data, the M23 abundance was increased in the plasma membrane (data not shown). The relative unit water permeability of the different isoforms was calculated based on the densitometry of the immunoblotting of the purified plasma membranes (Fig. 2g): 1.00 ± 0.00 for M1, 0.58 ± 0.06 for M23, and 0.73 ± 0.05 for Mz ($n = 3$ experiments, each based on $n = 5$ oocytes for L_p measurement and $n = 20$ oocytes for membrane preparation for each isoform), thus confirming the reduced relative unit water permeability of the M23 isoform.

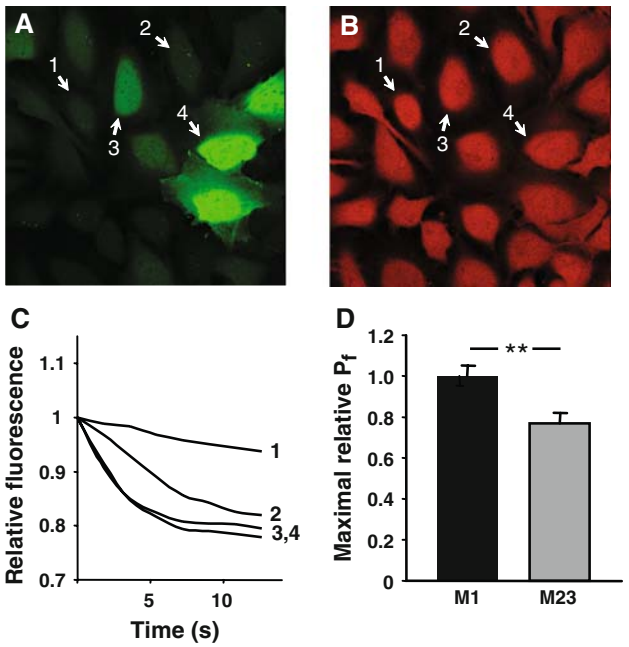

Fig. 3 The relative unit water permeability of M1 and M23 in transfected human bronchial epithelial cell line. **a** The level of GFP fluorescence within the cells. **b** Loading with calcein, which was used for water permeability measurements, was similar in AQP4-positive and AQP4-negative cells. *Numbers* indicate the same cells before (**a**) and after (**b**) calcein loading. **c** Single cell traces showing the dilution of calcein due to the cell swelling after an osmotic challenge. In cells with low GFP (and hence AQP4) expression (cells 1–3 in **a**), the swelling rate was increasing (*line 1* through *line 3* in **c**) with the increase in GFP (AQP4) level. The swelling of the cells 3 and 4 occurred at practically identical speed, probably due to saturation of the plasma membrane with AQP4. **d** Maximal relative water permeability in cells expressing M1 ($n = 22$) and M23 ($n = 13$), $^{**}P < 0.01$

Water permeability of AQP4 isoforms expressed in mammalian cells

To exclude the possibility that the reduced water permeability of M23 compared to M1 was specific to *Xenopus* oocytes as an expression system, we compared the relative water permeability of M1 and M23 in a bronchial epithelial cell line. The cells were transiently transfected with cDNA constructs that in each transfected cell produced two separate proteins, AQP4 and green fluorescent protein (GFP). GFP, which is a compact water soluble protein, was distributed throughout the cytoplasm and the nucleus of transfected cells (Fig. 3a). The cells with a weaker GFP signal demonstrated low water permeability, as judged from a low rate of swelling after hypoosmotic challenge (Fig. 3a, cell 1, and Fig. 3c, line 1). The cells with a stronger GFP signal had a higher water permeability (Fig. 3a, cells 2, 3, and Fig. 3c, lines 2, 3). With further increase in GFP expression, the rate of the swelling did not increase any further and the swelling of the cells 3 and 4 (Fig. 3a) occurred at practically identical speed (Fig. 3c), probably due to a saturation of the capacity of the plasma membrane to accommodate the water channels. The relative maximal P_f values that could be achieved in cells transfected with the M1 isoform were significantly higher than those in cells transfected with M23: 1.00 ± 0.05 for M1 ($n = 22$ cells) and 0.77 ± 0.05 for M23 ($n = 13$ cells), $P < 0.01$ (Fig. 3d).

Sensitivity to external K^+-concentration

To investigate a possible effect of K^+ on the water permeability of M1-, M23-, and Mz-expressing oocytes, we compared the water permeability in test solutions containing 8 mM KCl to the water permeability obtained in the presence of 2 mM KCl. In this experiment, oocytes had L_ps of (in $\times 10^{-3}$ cm/s) 1.63 ± 0.19 for M1, 2.38 ± 0.19 for M23, 1.37 ± 0.25 for Mz ($n = 5$ of each), and 0.10 ± 0.01 for non-injected oocytes ($n = 4$). The L_p of each oocyte was assessed at both K^+ concentrations and thereby served as its own control. The data are therefore presented as the ratio between the L_p obtained at 8 mM KCl and the L_p obtained at 2 mM KCl (Fig. 4). The water permeability of the three isoforms and the non-injected oocytes showed no significant degree of K^+-dependence; $L_{p(8K)}/L_{p(2K)}$: 0.98 ± 0.02 for M1, 1.01 ± 0.01 for M23, 1.05 ± 0.02 for Mz ($n = 5$ of each), and 1.02 ± 0.02 for non-injected oocytes ($n = 4$).

Solute permeability profile

To explore if M1-, M23-, or Mz-expressing oocytes were permeable to urea, glycerol, or formamide, we determined the L_p with 20 mOsm of each of these osmolytes and related them to the L_p obtained with the larger osmolyte, mannitol, to obtain the reflection coefficient, σ. These oocytes had L_ps of (in $\times 10^{-3}$ cm/s) 1.93 ± 0.12 for M1, 2.10 ± 0.41 for M23, 1.78 ± 0.33 for Mz ($n = 4$ of each), and 0.09 ± 0.02 for non-injected oocytes ($n = 3$). The reflection coefficients were identical for the three isoforms and the non-injected oocytes, which indicated that AQP4, independent of the isoform, was not permeable to these small molecules (Fig. 5a). The reflection coefficient was reduced for formamide, both for AQP4-expressing oocytes and for the non-injected oocytes, indicating that the native oocyte plasma membrane is slightly permeable to formamide. As a very low permeability to the osmolyte would not be detectable by this method, we performed uptake experiments using radio-labeled ^{14}C-mannitol, ^{14}C-urea, ^{14}C-glycerol, and ^{14}C-formamide (Fig. 5b). The pattern of the solute uptake by oocytes expressing M1, M23, Mz, and non-injected oocytes was identical to that observed for the reflection coefficients; expression of any of the three isoforms did not confer an increased permeability of the oocyte to any of these solutes ($n = 4$ experiments, 5 oocytes per condition).

PKC-dependent regulation

AQP4 is downregulated by PKC [8, 11, 35, 36] which we have found to be due to internalization of the protein [35].

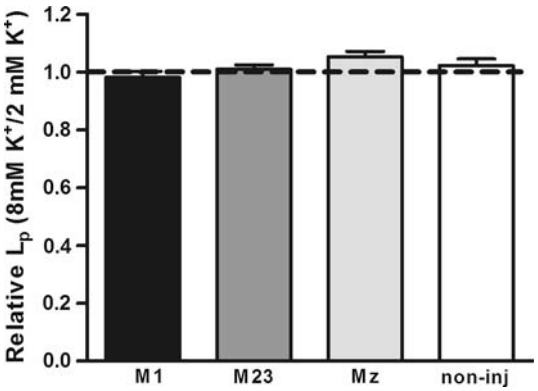

Fig. 4 Lack of K^+-dependent water permeability in M1, M23, and Mz-expressing oocytes. Oocytes expressing the three different isoforms were voltage-clamped to −50 mV to avoid K^+-dependent changes in membrane potential and exposed to test solution containing the standard 2 mM K^+ (+6 mM Ch^+) in which the L_p was determined. Subsequently the same oocyte was exposed to a test solution containing 8 mM K^+ in which the L_p was determined. The data are presented as the L_p obtained in 8 mM K^+ relative to that obtained in 2 mM K^+ ($n = 4$ of each)

Here, we investigated the rate of PKC-dependent downregulation of the three different isoforms. For each oocyte, the membrane-permeable PKC-activator, PMA (1 nM), was added to the test solution after determination of the oocyte basal water permeability. In this way, each oocyte was its own control and variations in the expression level did not affect the data. The L_p of the oocytes employed in this set of experiments was (in $\times 10^{-3}$ cm/s): 1.36 ± 0.07

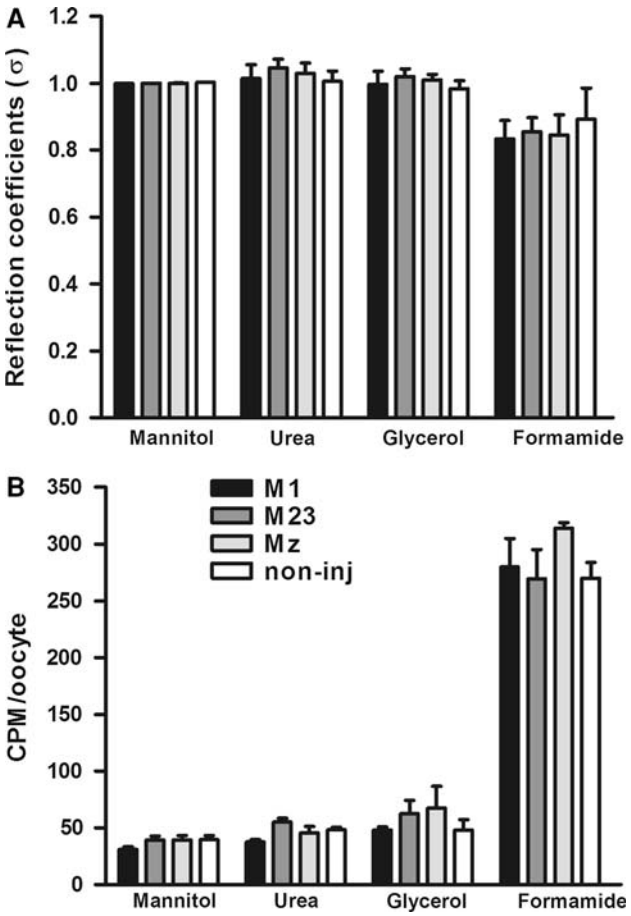

Fig. 5 Lack of permeability to small osmolytes in M1, M23, and Mz-expressing oocytes. **a** The L_p of oocytes expressing M1, M23, and Mz as well as non-injected oocytes was determined with different osmolytes; mannitol, urea, glycerol, and formamide (20 mOsm of each). The L_p obtained with urea, glycerol, and formamide was plotted relative to that obtained with mannitol for each oocyte (reflection coefficient, σ). The reflection coefficients for oocytes expressing M1, M23, or Mz were not significantly different from that of the non-injected oocytes ($n = 4$ of each isoform and $n = 3$ for the non-injected oocytes). **b** Oocytes expressing M1, M23, and Mz as well as non-injected oocytes were exposed to test solution containing different osmolytes; mannitol, urea, glycerol, and formamide (20 mOsm of each) in addition to trace amounts of the [^{14}C]-labeled osmolyte. The data are presented as the average uptake of four experiments performed in pentaplicate, with no significant difference between oocytes expressing the three isoforms and the non-injected oocytes

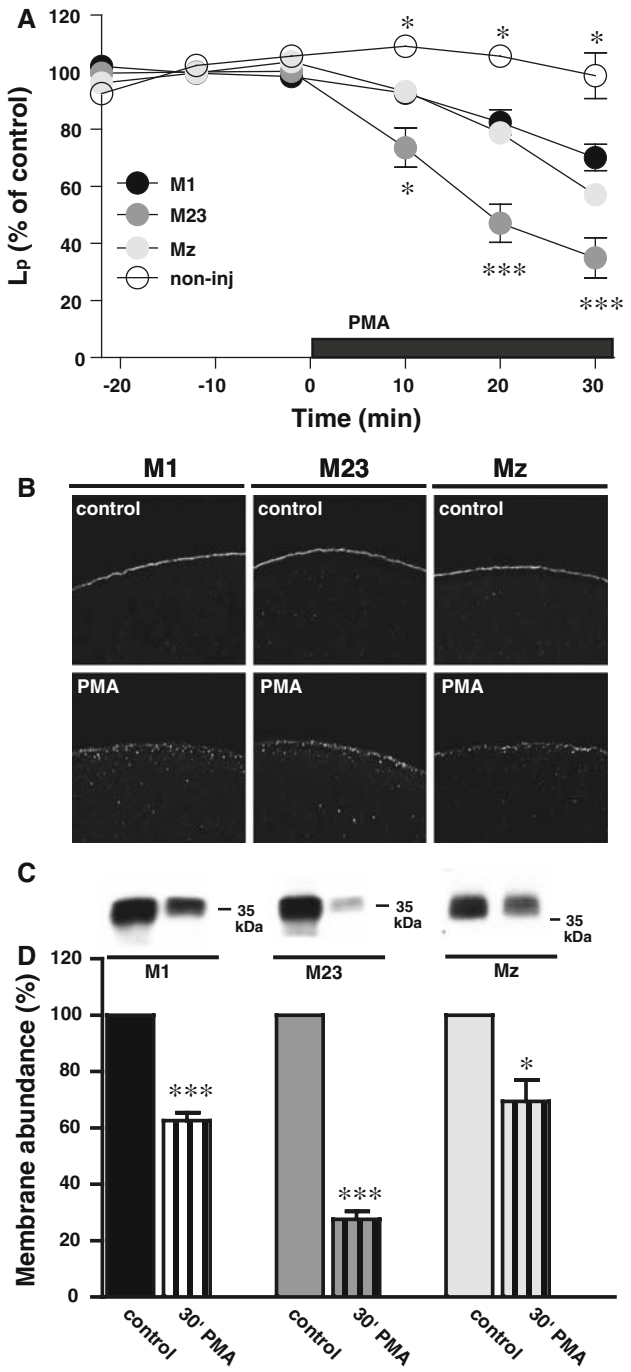

◀ **Fig. 6** PKC-dependent down-regulation of AQP4. **a** The relative water permeability of oocytes expressing M1, M23, or Mz or non-injected oocytes as a function of time. 1 nM PMA was included in the external solution as marked by the *black bar*. After 30 min of PMA treatment, the L_p was reduced to (in % of control) for M1; 70 ± 5 ($n = 8$), M23; 35 ± 7 ($n = 7$), Mz; 57 ± 4, error bar within the symbol ($n = 9$), and non-injected; 99 ± 8 ($n = 3$). The significance levels on the graph refer to M1, $^*P < 0.05$, $^{***}P < 0.001$. **b** Representative confocal laser scanning microscopy of oocytes expressing M1, M23, and Mz immunolabeled for AQP4 without (*upper panels*) or with (*lower panels*) 30 min PMA treatment (1 nM). **c** Representative immunoblot of plasma membrane purification of oocytes expressing M1, M23, or Mz in control condition and after 30 min of PMA treatment (1 nM), minimum 15 oocytes for each condition. **d** Relative membrane abundance of M1, M23, and Mz was assessed by densitometry of the immunoblots as presented in panel (**c**) of oocytes with control treatment or 30 min PMA treatment (1 nM). 15–20 oocytes were used for each condition ($n = 3$ experiments), $^*P < 0.05$, $^{***}P < 0.001$. The M23-expressing oocytes had a significantly lower AQP4 abundance in the plasma membrane after PMA treatment compared to M1 and Mz, $P < 0.01$

for M1 ($n = 8$), 1.40 ± 0.15 for M23 ($n = 8$), 1.19 ± 0.08 for Mz ($n = 9$), and 0.05 ± 0.01 for non-injected oocytes ($n = 3$). Figure 6a shows the PMA-dependent reduction of the L_p for the various isoforms of AQP4. The water permeability of oocytes expressing the three isoforms were down-regulated in response to PMA, but M23-expressing oocytes showed a faster and more pronounced down-regulation than M1- and Mz-expressing oocytes, with the non-injected oocytes being insensitive to PMA treatment. The significance levels on the graph refer to the M1 isoform. After 30 min of PMA treatment, the L_p was (in % of control); 70 ± 5 ($n = 8$) for M1, 35 ± 7 ($n = 7$) for M23, 57 ± 4 ($n = 9$) for Mz, and 99 ± 8 ($n = 3$) for the non-injected oocytes. To visualize the predicted PMA-dependent internalization of AQP4, immunocytochemistry was performed with the C-terminal anti-AQP4 antibody on oocytes expressing M1, M23, or Mz incubated for 30 min in control solution with or without 1 nM PMA ($n = 11$–14 of each). Representative confocal images clearly demonstrate appearance of AQP4 in intracellular vesicles, indicating PMA-dependent internalization of all three isoforms (Fig. 6b). In order to quantify the level of internalization, we prepared purified plasma membranes of M1-, M23-, and Mz-expressing oocytes after 30 min incubation in control solution with or without 1 nM PMA. The purified plasma membranes were immunoblotted with the anti-AQP4 antibody, representatives of which are shown in Fig. 6c. A summary of the densitometry is shown in Fig. 6d. After 30 min of PMA treatment, the amount of AQP4 left in the plasma membrane (in % of control) was 63 ± 3 for M1, 28 ± 3 for M23, and 69 ± 8 for Mz ($n = 3$ experiments with 15–20 oocytes for each condition per experiment). For all isoforms, PMA-dependent reduction in plasma membrane abundance was significantly different from control ($P < 0.001$ for M1 and M23 and $P < 0.05$ for Mz) and the PMA-dependent internalization of M23 was in addition significantly more pronounced than that of M1 and Mz ($P < 0.01$). PMA reduced the water permeability (Fig. 6a) and the membrane abundance of AQP4 (Fig. 6d) to the same extent for all three isoforms, suggesting that the effect of PKC on AQP4 may be due to the level of AQP4 internalization and not to a direct effect on channel function.

Discussion

In the present study, we investigated functional parameters of three isoforms of AQP4. All three isoforms were strictly permeable to water and did not allow permeation of smaller osmolytes, which is in agreement with previous studies performed on M1 and/or M23 [13, 34, 37], but has not previously been shown for Mz. The water permeability did not alter with the membrane potential and electrophysiological experiments were unable to detect any ionic conductance through either of the three isoforms (data not shown).

The large square arrays observed in freeze fracture replicas of perivascular glial endfeet [17] can be reconstituted in cell-line models by transfection of the M23 isoform of AQP4 [16, 18]. To validate the *Xenopus* expression system used here for functional comparison of AQP4 isoforms, it was necessary to investigate the formation of square arrays in this cell type. To this end, we performed freeze fracture studies of oocytes expressing the three isoforms. Expression of the M23 isoform in oocytes gave rise to square arrays, while the M1 or Mz failed to induce the formation of these higher order structures. To exclude the possibility that putative square arrays could have been overlooked in the M1- and Mz-expressing oocytes due to the membrane invaginations [28], we employed a newly developed biochemical assay for studying higher order AQP4 structures, BN-PAGE [20]. This method confirmed that M23, but not M1 and Mz, was organized in the high-molecular weight complexes when expressed in either *Xenopus* oocytes or HeLa cells. Taken together, our freeze fracture and BN-PAGE experiments validated our use of *Xenopus* oocytes for functional analysis of the three AQP4 isoforms.

The relative unit water permeability of the M1 and M23 isoforms has been debated in several studies. Experiments using heterologous expression of M1 and M23 in *Xenopus* oocytes have demonstrated identical water permeability of oocytes expressing M1 or M23 [13, 15], although the membrane abundance of AQP4 was not quantified in these studies. A conflicting study has reported an eightfold higher water permeability of the M23 isoform compared to the M1 isoform LLC-PK1 cells [25]. Comparative determination of the water permeability in the latter study may have been complicated by the large variability in size of the LLC-PK1 cells, which was dependent on the AQP4 isoform expressed, and the fact that the calculation of the water permeability was based on an assumption of the LLC-PK1 cells being spherical. In the present study, the overall water permeability of oocytes expressing the different AQP4 isoforms was similar, which is in agreement with the previous studies performed on *Xenopus* oocytes [13, 15]. In addition, the *total* abundance of AQP4 was similar for the three isoforms, although the M23 isoform had a significantly higher *plasma membrane* abundance compared to the other isoforms. The plasma membrane abundance was assessed with immunocytochemistry as well as with immunoblotting of purified plasma membranes to rule out possible isoform-specific differences in antibody binding, i.e., steric hindrance upon square array formation. Relating the water permeability of M1-, M23-, and Mz-expressing oocytes to the amount of AQP4 in the plasma membrane revealed that the relative unit water permeability of the M23 isoform was $\sim$40% lower than that of M1 while Mz was intermediate in its water permeability ($\sim$20% lower than M1).

To exclude the possibility that the lower relative water permeability of M23 was specific to the oocyte expression system, the difference between the water permeability of M1 and M23 was investigated in a mammalian expression system. In these experiments, the maximal water permeability of M23-expressing cells was also lower than that of M1-expressing cells, which is in agreement with our oocyte data. However, the membrane abundance of the two isoforms was not quantified in this set of data nor in a previous study on COS-7 cells transfected with c-myc-tagged M1 or M23 [19] in which a similar result was obtained. Taken together, in contrast to [25], but in agreement with [19], our results suggest that the unit water permeability of M23 is lower than the other isoforms.

In astrocytes and retinal Müller cells, AQP4 is extensively co-localized with the inwardly rectifying K^+ channel Kir4.1 [38, 39]. The co-localization of a K^+ channel with an aquaporin has warranted suggestions that AQP4 might facilite K^+ clearance from the perisynaptic space [38, 39]. To that effect, it has indeed been shown that mice lacking either AQP4 itself [40] or the endfoot-specific localization of AQP4 [41] had a slower K^+ clearance and therefore more intense and longer lasting experimentally induced seizures. However, the functional characteristics of Kir4.1 in freshly isolated glial cells were not altered by genetic deletion of AQP4, which suggests that Kir4.1 is not directly affected by its co-localization with AQP4 [42, 43]. Our recent studies showed that Kir4.1 was activated by cell swelling, and that AQP4 thereby may pose an indirect effect on the activity of Kir4.1 [44]. The question then arose if the water permeability of AQP4 could be affected by the increase in external K^+ concentration that inevitably leads to glial cell swelling [45, 46]. Increasing the K^+ concentration in the test solution from 2 to 8 mM did not alter the water permeability of M1-, M23-, or Mz-expressing oocytes, which bears evidence of AQP4 being insensitive to increase in external K^+ concentration (at least in the range tested).

AQP4 is regulated by several protein kinases with various effects on the protein, such as gating, internalization,

trafficking to the plasma membrane, and lysosomal targeting [5–11]. PKC has been shown to phosphorylate AQP4 directly in rat brain homogenate [8] and in AQP4-expressing glioma cells [36], although this was not apparent in mouse primary cultured astrocytes [9]. PKC activation down-regulates the water permeability of AQP4 expressed in a mammalian cell line, glioma cells, or in *Xenopus* oocytes [8, 11, 35, 36]. We recently showed that the PKC-dependent reduction of the water permeability of AQP4-expressing *Xenopus* oocytes was due to internalization of AQP4 [35]. In the present study, it was evident that the water permeability of the M23-expressing oocytes was significantly more sensitive to PKC activation than oocytes expressing the longer isoforms. Importantly, PKC-dependent AQP4 internalization was also more prominent with the M23 isoform. There was no significant difference between the PMA-dependent reduction in water permeability and the PMA-dependent level of internalization for any of the three isoforms, suggesting that the effect of PKC on AQP4 is primarily due to the level of AQP4 internalization and not to a direct effect on channel function. The increased PKC sensitivity of the M23 isoform suggests a function for the organization of AQP4 isoforms into large square arrays. One may speculate that, after phosphorylation of AQP4, the internalization machinery will be able to retrieve more units of AQP4 per unit of adaptor proteins if AQP4 is organized into square arrays. The more efficient internalization of large amounts of AQP4 with square arrays would thus increase dynamic regulation of AQP4 in vivo, and therefore we may have revealed the first functional rationale for maintaining the elaborate square arrays. Disruption of square arrays in the glial endfeet within minutes after the onset of cerebral ischemia has indeed been demonstrated [47–49], although a conflicting study identifies square arrays present in the astrocytic endfeet 60 min after the onset of hypoxia [50]. One may speculate whether the putative hypoxia-induced disruption of square arrays may be indicative of phosphorylation-dependent internalization of AQP4, i.e., via the G-protein coupled vasopressin receptor, $V1_aR$ [35].

Acknowledgments Technical assistance was provided by Charlotte G. Iversen, Mikkel Olsen, and Inger Merete Paulsen. The authors wish to give special thanks to Karen Thomsen for expert freeze fracture studies. The study was supported by the Nordic Centre of Excellence in Water-Imbalance Related Disorders, the Lundbeck Foundation (to N.M.), the Danish Medical Research Council (FSS) (to N.M., R.A.F.), E. Danielsen's Foundation (to N.M.), the Augustinus Foundation (to N.M.), the Michaelsen's Foundation (to N.M.), the Novo Nordisk Foundation (to R.A.F.), the Carlsberg Foundation (to R.A.F.) and the L'Oreal/UNESCO/Royal Danish Academy of Sciences Scholarship to Young Women in Science (to N.M.), Heart–Lung Foundation (to M.Z.), and the Functional genomics program of the Norwegian Research Council, FUGE (to T.H.). Additional funding to R.A.F was provided by a Marie Curie Intra-European Fellowship. The Water and Salt Research Center at the University of Aarhus is established and supported by the Danish National Research Foundation (Danmarks Grundforskningsfond).

References

1. Amiry-Moghaddam M, Ottersen OP (2003) The molecular basis of water transport in the brain. Nat Rev Neurosci 4:991–1001
2. Nielsen S, Nagelhus EA, Amiry-Moghaddam M, Bourque C, Agre P, Ottersen OP (1997) Specialized membrane domains for water transport in glial cells: high-resolution immunogold cytochemistry of aquaporin-4 in rat brain. J Neurosci 17:171–180
3. Noell S, Fallier-Becker P, Beyer C, Kroger S, Mack AF, Wolburg H (2007) Effects of agrin on the expression and distribution of the water channel protein aquaporin-4 and volume regulation in cultured astrocytes. Eur J Neurosci 26:2109–2118
4. Zador Z, Stiver S, Wang V, Manley GT (2009) Role of aquaporin-4 in cerebral edema and stroke. Handb Exp Pharmacol 190:159–170
5. Carmosino M, Procino G, Tamma G, Mannucci R, Svelto M, Valenti G (2007) Trafficking and phosphorylation dynamics of AQP4 in histamine-treated human gastric cells. Biol Cell 99:25–36
6. Gunnarson E, Axehult G, Baturina G, Zelenin S, Zelenina M, Aperia A (2005) Lead induces increased water permeability in astrocytes expressing aquaporin 4. Neuroscience 136:105–114
7. Gunnarson E, Zelenina M, Axehult G, Song Y, Bondar A, Krieger P, Brismar H, Zelenin S, Aperia A (2008) Identification of a molecular target for glutamate regulation of astrocyte water permeability. Glia 56:587–596
8. Han Z, Wax MB, Patil RV (1998) Regulation of aquaporin-4 water channels by phorbol ester-dependent protein phosphorylation. J Biol Chem 273:6001–6004
9. Kadohira I, Abe Y, Nuriya M, Sano K, Tsuji S, Arimitsu T, Yoshimura Y, Yasui M (2008) Phosphorylation in the C-terminal domain of aquaporin-4 is required for Golgi transition in primary cultured astrocytes. Biochem Biophys Res Commun 377:463–468
10. Madrid R, Le MS, Barrault MB, Janvier K, Benichou S, Merot J (2001) Polarized trafficking and surface expression of the AQP4 water channel are coordinated by serial and regulated interactions with different clathrin-adaptor complexes. EMBO J 20:7008–7021
11. Zelenina M, Zelenin S, Bondar AA, Brismar H, Aperia A (2002) Water permeability of aquaporin-4 is decreased by protein kinase C and dopamine. Am J Physiol Ren Physiol 283:F309–F318
12. Hasegawa H, Ma T, Skach W, Matthay MA, Verkman AS (1994) Molecular cloning of a mercurial-insensitive water channel expressed in selected water-transporting tissues. J Biol Chem 269:5497–5500
13. Jung JS, Bhat RV, Preston GM, Guggino WB, Baraban JM, Agre P (1994) Molecular characterization of an aquaporin cDNA from brain: Candidate osmoreceptor and regulator of water balance. Proc Natl Acad Sci USA 91:13052–13056
14. Moe SE, Sorbo JG, Sogaard R, Zeuthen T, Ottersen OP, Holen T (2008) New isoforms of rat aquaporin-4. Genomics 91:367–377
15. Neely JD, Christensen BM, Nielsen S, Agre P (1999) Heterotetrameric composition of aquaporin-4 water channels. Biochemistry 38:11156–11163
16. Furman CS, Gorelick-Feldman DA, Davidson KG, Neely Yasumura T, JD Agre P, Rash JE (2003) Aquaporin-4 square array assembly: opposing actions of M1 and M23 isoforms. Proc Natl Acad Sci USA 100:13609–13614
17. Rash JE, Yasumura T, Hudson CS, Agre P, Nielsen S (1998) Direct immunogold labeling of aquaporin-4 in square arrays of

astrocyte and ependymocyte plasma membranes in rat brain and spinal cord. Proc Natl Acad Sci USA 95:11981–11986
18. Yang B, Brown D, Verkman AS (1996) The mercurial insensitive water channel (AQP-4) forms orthogonal arrays in stably transfected Chinese hamster ovary cells. J Biol Chem 271:4577–4580
19. Crane JM, Van Hoek AN, Skach WR, Verkman AS (2008) Aquaporin-4 dynamics in orthogonal arrays in live cells visualized by quantum dot single particle tracking. Mol Biol Cell 19:3369–3378
20. Sorbo JG, Moe SE, Ottersen OP, Holen T (2008) The molecular composition of square arrays. Biochemistry 47:2631–2637
21. Strand L, Moe SE, Solbu TT, Vaadal M, Holen T (2009) Roles of aquaporin-4 isoforms and amino acids in square array assembly. Biochemistry 48:5785–5793
22. Suzuki H, Nishikawa K, Hiroaki Y, Fujiyoshi Y (2008) Formation of aquaporin-4 arrays is inhibited by palmitoylation of N-terminal cysteine residues. Biochim Biophys Acta 1778:1181–1189
23. Crane JM, Verkman AS (2009) Determinants of aquaporin-4 assembly in orthogonal arrays revealed by live-cell single-molecule fluorescence imaging. J Cell Sci 122:813–821
24. Hiroaki Y, Tani K, Kamegawa A, Gyobu N, Nishikawa K, Suzuki H, Walz T, Sasaki S, Mitsuoka K, Kimura K, Mizoguchi A, Fujiyoshi Y (2006) Implications of the aquaporin-4 structure on array formation and cell adhesion. J Mol Biol 355:628–639
25. Silberstein C, Bouley R, Huang Y, Fang P, Pastor-Soler N, Brown D, Van Hoek AN (2004) Membrane organization and function of M1 and M23 isoforms of aquaporin-4 in epithelial cells. Am J Physiol Ren Physiol 287:F501–F511
26. Zeidel ML, Nielsen S, Smith BL, Ambudkar SV, Maunsbach AB, Agre P (1994) Ultrastructure, pharmacologic inhibition, and transport selectivity of aquaporin channel-forming integral protein in proteoliposomes. Biochemistry 33:1606–1615
27. Zeuthen T, Belhage B, Zeuthen E (2006) Water transport by Na+-coupled cotransporters of glucose (SGLT1) and of iodide (NIS). The dependence of substrate size studied at high resolution. J Physiol 570:485–499
28. Zampighi GA, Kreman M, Boorer KJ, Loo DD, Bezanilla F, Chandy G, Hall JE, Wright EM (1995) A method for determining the unitary functional capacity of cloned channels and transporters expressed in *Xenopus laevis* oocytes. J Membr Biol 148:65–78
29. Leduc-Nadeau A, Lahjouji K, Bissonnette P, Lapointe JY, Bichet DG (2007) Elaboration of a novel technique for purification of plasma membranes from *Xenopus laevis* oocytes. Am J Physiol Cell Physiol 292:C1132–C1136
30. Moeller HB, MacAulay N, Knepper MA, Fenton RA (2009) Role of multiple phosphorylation sites in the COOH-terminal tail of aquaporin-2 for water transport: evidence against channel gating. Am J Physiol Ren Physiol 296:F649–F657
31. Fenton RA, Brond L, Nielsen S, Praetorius J (2007) Cellular and subcellular distribution of the type-2 vasopressin receptor in the kidney. Am J Physiol Ren Physiol 293:F748–F760
32. Zelenina M, Bondar AA, Zelenin S, Aperia A (2003) Nickel and extracellular acidification inhibit the water permeability of human aquaporin-3 in lung epithelial cells. J Biol Chem 278:30037–30043
33. Zelenina M, Brismar H (2000) Osmotic water permeability measurements using confocal laser scanning microscopy. Eur Biophys J 29:165–171
34. Yang B, Verkman AS (1997) Water and glycerol permeabilities of aquaporin 1–5 and MIP determined quantitatively by expression of epitope-tagged constructs in *Xenopus* oocytes. J Biol Chem 272:16140–16146
35. Moeller HB, Fenton RA, Zeuthen T, MacAulay N (2009) Vasopressin-dependent short-term regulation of AQP4 expressed in *Xenopus* oocytes. Neuroscience 164:1674–1684
36. McCoy ES, Haas BR, Sontheimer H (2009) Water permeability through aquaporin-4 is regulated by protein kinase C and becomes rate-limiting for glioma invasion. Neuroscience (in press)
37. Meinild AK, Klaerke DA, Zeuthen T (1998) Bidirectional water fluxes and specificity for small hydrophilic molecules in aquaporins 0–5. J Biol Chem 273:32446–32451
38. Nagelhus EA, Horio Y, Inanobe A, Fujita A, Haug FM, Nielsen S, Kurachi Y, Ottersen OP (1999) Immunogold evidence suggests that coupling of K+ siphoning and water transport in rat retinal Muller cells is mediated by a coenrichment of Kir4.1 and AQP4 in specific membrane domains. Glia 26:47–54
39. Nagelhus EA, Mathiisen TM, Ottersen OP (2004) Aquaporin-4 in the central nervous system: cellular and subcellular distribution and coexpression with KIR4.1. Neuroscience 129:905–913
40. Binder DK, Yao X, Zador Z, Sick TJ, Verkman AS, Manley GT (2006) Increased seizure duration and slowed potassium kinetics in mice lacking aquaporin-4 water channels. Glia 53:631–636
41. Amiry-Moghaddam M, Williamson A, Palomba M, Eid T, de Lanerolle NC, Nagelhus EA, Adams ME, Froehner SC, Agre P, Ottersen OP (2003) Delayed K+ clearance associated with aquaporin-4 mislocalization: phenotypic defects in brains of alpha-syntrophin-null mice. Proc Natl Acad Sci USA 100:13615–13620
42. Ruiz-Ederra J, Zhang H, Verkman AS (2007) Evidence against functional interaction between aquaporin-4 water channels and Kir4.1 potassium channels in retinal Muller cells. J Biol Chem 282:21866–21872
43. Zhang H, Verkman AS (2008) Aquaporin-4 independent Kir4.1 K+ channel function in brain glial cells. Mol Cell Neurosci 37:1–10
44. Soe R, MacAulay N, Klaerke DA (2009) Modulation of Kir4.1 and Kir4.1-Kir5.1 channels by small changes in cell volume. Neurosci Lett 457:80–84
45. MacVicar BA, Feighan D, Brown A, Ransom B (2002) Intrinsic optical signals in the rat optic nerve: role for K(+) uptake via NKCC1 and swelling of astrocytes. Glia 37:114–123
46. Walz W, Hinks EC (1985) Carrier-mediated KCl accumulation accompanied by water movements is involved in the control of physiological K+ levels by astrocytes. Brain Res 343:44–51
47. Cuevas P, Gutierrez Diaz JA, Dujovny M, Diaz FG, Ausman JI (1985) Disturbance of plasmalemmal astrocytic assemblies in focal and selective cerebral ischemia. Anat Embryol (Berl) 172:171–175
48. Landis DM, Reese TS (1981) Astrocyte membrane structure: changes after circulatory arrest. J Cell Biol 88:660–663
49. Suzuki M, Iwasaki Y, Yamamoto T, Konno H, Yoshimoto T, Suzuki J (1984) Disintegration of orthogonal arrays in perivascular astrocytic processes as an early event in acute global ischemia. Brain Res 300:141–145
50. Neuhaus J, Schmid EM, Wolburg H (1990) Stability of orthogonal arrays of particles in murine skeletal muscle and astrocytes after circulatory arrest, and human gliomas. Neurosci Lett 109:163–168